The interaction between the ER membrane protein UNC93B and TLR3, 7, and 9 is crucial for TLR signaling

Melanie M. Brinkmann,[1] Eric Spooner,[1] Kasper Hoebe,[2] Bruce Beutler,[2] Hidde L. Ploegh,[1] and You-Me Kim[1]

[1]Whitehead Institute for Biomedical Research, Cambridge, MA 02142
[2]Department of Immunology, The Scripps Research Institute, La Jolla, CA 92037

Toll-like receptors (TLRs) sense the presence of microbial and viral pathogens by signal transduction mechanisms that remain to be fully elucidated. A single point mutation (H412R) in the polytopic endoplasmic reticulum (ER)–resident membrane protein UNC93B abolishes signaling via TLR3, 7, and 9. We show that UNC93B specifically interacts with TLR3, 7, 9, and 13, whereas introduction of the point mutation H412R in UNC93B abolishes their interactions. We establish the physical interaction of the intracellular TLRs with UNC93B in splenocytes and bone marrow–derived dendritic cells. Further, by expressing chimeric TLRs, we show that TLR3 and 9 bind to UNC93B via their transmembrane domains. We propose that a physical association between UNC93B and TLRs in the ER is essential for proper TLR signaling.

Introduction

Toll-like receptors (TLRs) are involved in the recognition and processing of a variety of signals delivered by viral and microbial products (Janeway and Medzhitov, 2002; Takeda et al., 2003). TLRs sense the presence of molecules that are broadly conserved across microbial taxa. TLR activation initiates the innate immune response by inducing the expression of antimicrobial genes and inflammatory cytokines. Activation of TLRs also enhances adaptive immunity through activation of dendritic cells. TLR-mediated recognition of microbial components by dendritic cells induces the expression of costimulatory molecules, such as CD80/CD86, and the secretion of inflammatory cytokines, and it is responsible for the rearrangement of trafficking pathways of class II major histocompatability complex (MHC) products (Akira et al., 2001; Iwasaki and Medzhitov, 2004). There are 10 and 12 TLR paralogues in humans and mice, respectively. Both species have TLR1–9. Mice lack TLR10, but have TLR11–13, which humans lack. Each TLR appears to sense the presence of distinct microbial components (Takeda et al., 2003; Kawai and Akira, 2006). For example, TLR4 recognizes lipopolysaccharides (LPSs), which are components of the Gram-negative bacterial outer membrane, whereas double-stranded RNA, single-stranded RNA, and unmethylated bacterial DNA (CpG) engage TLR3, 7, and 9, respectively (Poltorak et al., 1998; Hemmi et al., 2000; Alexopoulou et al., 2001; Bauer et al., 2001; Diebold et al., 2004; Heil et al., 2004).

Mutations affecting TLR-mediated cellular responses have been instrumental in delineating the components of the relevant signal transduction cascades (Beutler et al., 2006). These include spontaneous mutations, targeted gene disruptions, and chemically induced mutations, the best characterized of which include the deficiencies in MyD88 and TRIF adaptor molecules (Kawai et al., 1999; Hoebe et al., 2003) and in the kinases that act downstream of them (Suzuki et al., 2002; Shim et al., 2005; Hoshino et al., 2006). In a forward genetic screen using mutagenesis with *N*-ethyl-*N*-nitrosourea, Tabeta et al. (2006) identified "triple D" (3d) mice that showed defects in TLR3, 7, and 9 signaling, as well as in class I and II MHC-restricted antigen presentation. The mutation was identified as a single histidine-to-arginine substitution (H412R) in the polytopic membrane protein UNC93B. Mice carrying this mutation are highly susceptible to infection with mouse cytomegalovirus, *Listeria monocytogenes*, and *Staphylococcus aureus*. Notably, the histidine residue affected in the UNC93B mutation is invariant for all vertebrate orthologues. UNC93B deficiency has also been linked to the etiology of herpes simplex virus-1 encephalitis in human patients (Casrouge et al., 2006). Similar to what

Correspondence to Hidde L. Ploegh: ploegh@wi.mit.edu; or You-Me Kim: ykim@wi.mit.edu

Abbreviations used in this paper: ATCC, American Type Culture Collection; BM-DC, bone marrow–derived dendritic cell; HEK, human embryonic kidney; HIFS, heat-inactivated fetal calf serum; LPS, lipopolysaccharide; MHC, major histocompatibility complex; MS, mass spectrometry; TEV, Tobacco Etch virus; TIR, Toll-interleukin 1 receptor; TLR, Toll-like receptor.

The online version of this article contains supplemental material.

The Journal of Cell Biology, Vol. 177, No. 2, April 23, 2007 265–275
http://www.jcb.org/cgi/doi/10.1083/jcb.200612056

was observed in 3d mice, cells from patients with a mutation in the *Unc93b1* gene show impaired cytokine production upon stimulation of TLR3, 7, 8, and 9 and are highly susceptible to various viral infections.

The molecular mechanisms that underlie the immunological defects in the UNC93B mutant mice and in human patients are not known. Moreover, no specific function has been assigned to UNC93B. In *Caenorhabditis elegans*, *Unc93*, which is the founding member and sole homologue of mammalian *Unc93b*, encodes a regulatory subunit of a two-pore potassium channel complex and plays a role in coordinated muscle contraction (Greenwald and Horvitz, 1980; Levin and Horvitz, 1992; de la Cruz et al., 2003). Multiple paralogues of UNC93 exist in mammals, two of which are UNC93A (32% amino acid identity to *C. elegans* UNC93) and UNC93B (20% amino acid identity to *C. elegans* UNC93). UNC93A and UNC93B are highly conserved between human and mouse (71% amino acid identity for UNC93A and 90% amino acid identity for UNC93B). Human UNC93A and UNC93B are predicted multispanning transmembrane proteins and the GFP fusion protein of human UNC93A localizes to the plasma membrane (Kashuba et al., 2002; Liu et al., 2002). Mammalian UNC93B contains a domain of unknown function (DUF895) between residues 124 and 189, and human UNC93B shows a weak homology to the bacterial ABC-2 type transporter signature between residues 319 and 523 (Kashuba et al., 2002; Tabeta et al., 2006). However, no functional role has been established for such domains.

We analyzed the biosynthesis and maturation of murine UNC93B and discovered that wild-type, but not mutant, UNC93B physically interacts with TLR3, 7, 9, and 13, as assessed by mass spectrometry (MS) and biochemical approaches. Using genetic and immunochemical tools, we further confirmed the interaction between endogenous UNC93B and TLRs in primary dendritic cells and splenocytes of wild-type mice, but not UNC93B mutant mice. The essential role for UNC93B in TLR signaling is thus explained by direct interactions with its client TLRs.

Results

Wild-type and mutant UNC93B proteins retain Endo H sensitivity and show similar stability

The murine *Unc93b* gene comprises 11 exons and gives rise to a protein of 598 amino acids. Topology prediction programs suggest that UNC93B spans the membrane 12 times, and the 3d mutation (H412R) is located within transmembrane domain 9 (Fig. 1 A). UNC93B has two putative N-linked glycosylation sites (consensus NxS/T), $N^{251}HT$ and $N^{272}KT$ (Fig. 1 A). We raised polyclonal rabbit antibodies against several peptide sequences of the N- and C-terminal portions of UNC93B. The antibodies showed reactivity with both wild-type and mutant UNC93B, as assessed by immunoblotting and immunoprecipitation on cell extracts prepared from a variety of sources (unpublished data).

Polar residues in transmembrane domains are involved in helix–helix interactions within a multitransmembrane domain–containing protein to aid helix packing or participate in protein–protein interactions with a neighboring membrane protein (Curran and Engelman, 2003). Missense mutations involving the loss or gain of an arginine residue in a predicted transmembrane domain are often associated with protein misfolding and malfunction, as found in many human diseases (Partridge et al., 2004). Therefore, we assessed the effects of the H412R mutation on expression, maturation, and stability of the UNC93B protein. We generated an epitope-tagged version of UNC93B in which the Flag-Tobacco Etch virus (TEV)-HA tag was attached to the C terminus of either the wild-type (UNC93B-HA WT) or mutant (UNC93B-HA H412R) UNC93B protein (Fig. 1 A). We then introduced epitope-tagged wild-type and mutant UNC93B into the macrophage cell line RAW 264.7 and conducted pulse-chase experiments. Wild-type and mutant UNC93B-HA showed similar half-lives (~4 h), but exhibited distinct migration patterns in SDS-PAGE (Fig. 1 B). Wild-type UNC93B migrates as heterodisperse material upon SDS-PAGE, whereas the UNC93B mutant form is dominated by a well-defined distinct polypeptide in addition to more diffuse material (Fig. 1 B).

To rule out the possibility that the distinct polypeptide seen for mutant UNC93B represents a protein that associates with mutant UNC93B rather than the mutant protein itself, we performed immunoprecipitation experiments with the polyclonal antiserum directed against the C-terminal segment of UNC93B (anti–UNC-C), followed by reimmunoprecipitation experiments with an UNC93B antibody raised against the N terminus (anti–UNC-N), anti-HA, or anti-Flag antibodies. We recovered epitope-tagged, as well as endogenous, UNC93B from RAW macrophages with the anti–UNC-C antiserum (Fig. 1c). Reimmunoprecipitation with anti–UNC-N antiserum after mild denaturation of the initial immunoprecipitation samples recovered endogenous, as well as epitope-tagged, UNC93B, whereas anti-HA and -Flag monoclonal antibodies recovered only epitope-tagged UNC93B proteins, as expected (Fig. 1 C). The distinctly migrating polypeptide of mutant UNC93B was also recovered by reimmunoprecipitation (Fig. 1 C), confirming that it derives from the UNC93B protein and not from a separate UNC93B-associated polypeptide.

To examine the maturation of endogenous wild-type and mutant UNC93B proteins, we performed pulse-chase analysis of bone marrow–derived dendritic cells (BM-DCs) from wild-type (C57BL/6) and UNC93B mutant (3d) mice. We confirmed the 3d phenotype of the UNC93B mutant mice through measurement of TNF production in BM-DCs after stimulation with TLR agonists. As reported, cells from 3d mice showed a complete lack of response to TLR7 and 9 agonists, whereas the response to the TLR4 agonist LPS was not affected (Fig. S1, available at http://www.jcb.org/cgi/content/full/jcb.200612056/DC1). The cells were first labeled with [^{35}S]methionine/cysteine for 30 min. After chase periods of 0, 1, and 4 h, endogenous UNC93B was recovered by immunoprecipitation with the anti–UNC-C antiserum. The immunoprecipitates were subjected to glycosidase digestion. In agreement with the proposed intracellular location of UNC93B as an ER-localized protein (Tabeta et al., 2006), we found that both wild-type and mutant UNC93B proteins recovered during the entire chase period retained full sensitivity to Endoglycosidase H (Endo H; Fig. 1 D). Immunofluorescence

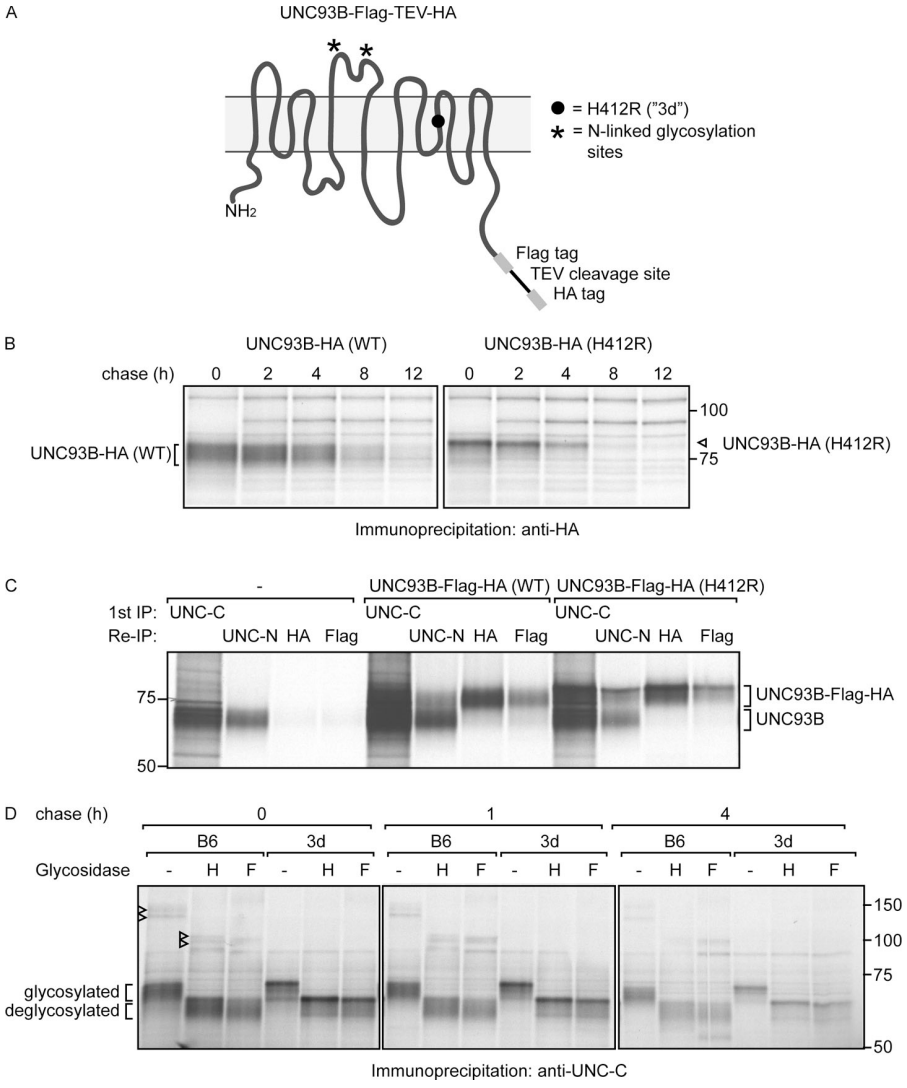

Figure 1. **Characterization of wild-type and mutant UNC93B proteins.** (A) Model of the UNC93B protein. The single point mutation of histidine residue 412 to arginine (H412R, 3d mutation) is located within transmembrane domain 9 (•). The two predicted N-linked glycosylation sites ($N^{251}HT$ and $N^{272}KT$) are indicated (*). Wild-type and mutant (H412R) UNC93B were fused at the C terminus with a Flag tag, followed by the TEV protease cleavage site and an HA-tag (designated as UNC93B-HA). (B) RAW macrophages stably expressing epitope-tagged wild-type UNC93B-HA (WT, left) or mutant UNC93B-HA (H412R, right) were metabolically labeled with [^{35}S]methionine/cysteine for 30 min (pulse) and lysed in RIPA buffer after 0, 2, 4, 8, and 12 h of incubation in normal medium (chase). UNC93B proteins were recovered by immunoprecipitation with an anti-HA antibody and resolved by SDS-PAGE. Wild-type and mutant UNC93B proteins show similar stability, but differ in their migration patterns; wild-type UNC93B migrates as heterodispersed material on SDS-PAGE, whereas the UNC93B mutant form migrates as a well-defined distinct polypeptide in addition to more diffuse material. (C) Endogenous and epitope-tagged UNC93B proteins were immunoprecipitated in 1% NP-40 lysis buffer from ^{35}S-labeled RAW macrophages that are nontransduced (–) or transduced with UNC93B-HA (WT) or UNC93B-HA (H412R) using a polyclonal antibody directed against the C terminus of UNC93B (anti–UNC-C). Reimmunoprecipitations were performed after mild denaturation of the initial immunoprecipitation with a polyclonal antiserum against the N terminus of UNC93B (anti–UNC-N) or antibodies to the HA or Flag epitopes. Recovered epitope-tagged and endogenous UNC93B proteins were resolved by SDS-PAGE. The distinct polypeptide observed in direct immunoprecipitations of mutant UNC93B is also observed after reimmunoprecipitation of mutant UNC93B, and is thus UNC93B itself. (D) BM-DCs from either wild-type C57BL/6 (B6) or UNC93B mutant (3d) mice were pulsed with [^{35}S]methionine/cysteine for 40 min and lysed in 1% digitonin lysis buffer after 0, 1, or 4 h of incubation in normal medium (chase). Endogenous UNC93B proteins were immunoprecipitated with the affinity purified anti–UNC-C antibody, subjected to digestion with glycosidases Endo H (H) or PNGase F (F) or not digested (–), and resolved by SDS-PAGE. Both wild-type and mutant UNC93B proteins retain full sensitivity to Endo H digestion. The polypeptides migrating at the range of 130–150 kD in nondigested samples and at ~100 kD in Endo H/PNGase F-digested samples (arrowheads) are only present in wild-type samples, but not in the 3d samples (Fig. 3 A and Fig. 6 A).

analysis of wild-type and mutant UNC93B-HA with an anti-HA monoclonal antibody in paraformaldehyde-fixed RAW cells resulted in a reticular membrane staining pattern that closely overlaps with staining pattern for the ER membrane protein calnexin, confirming ER localization of both wild-type and mutant UNC93B (unpublished data).

Notably, the endogenous UNC93B mutant protein recovered from 3d mice showed the same discrete polypeptide, in addition to the presence of diffuse material, whereas wild-type UNC93B only showed the heterodispersed band (Fig. 1 D). As observed for epitope-tagged UNC93B, endogenous UNC93B is a stable protein, and wild-type and mutant UNC93B do not show any difference in stability. These results further show that tagging UNC93B at its C terminus does not necessarily influence its maturation or stability.

From these experiments, we conclude that the phenotype observed in the UNC93B mutant mice neither results from the lack of UNC93B protein expression nor can it be attributed to a shortened half-life of the mutant UNC93B protein. Further, both wild-type and mutant UNC93B retain full Endo H sensitivity, which is consistent with their localization to the ER.

Maturation of MHC products is normal in BM-DCs from 3d mice

The 3d mice not only show a defect in TLR signaling via TLR3, 7, and 9 but are also compromised in their ability to engage in cross-presentation via class I MHC molecules and in class II MHC-restricted antigen presentation (Tabeta et al., 2006). Even though surface levels of MHC products at steady state may not be affected by the 3d mutation, this leaves open the possibility of alterations in their trafficking. We performed pulse-chase analysis for class I and II MHC products on BM- DCs obtained from wild-type and 3d mice. Maturation of class II MHC molecules was examined by assessing the levels of SDS-stable, peptide-loaded

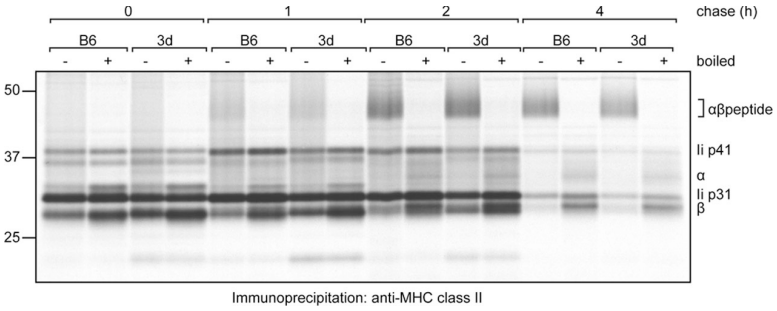

Figure 2. **Maturation of MHC class II is not altered in UNC93B mutant mice.** BM-DCs from either wild-type C57BL/6 (B6) or UNC93B mutant (3d) mice were pulsed with [^{35}S]methionine/cysteine for 40 min and lysed in 1% digitonin lysis buffer after 0, 1, 2, or 4 h of incubation in normal medium (chase). Endogenous MHC class II was immunoprecipitated with the anti-MHC class II antibody (N22). Immunoprecipitates were loaded under denaturing (boiled) or mildly denaturing (nonboiled) conditions and resolved by SDS-PAGE. SDS-stable class II MHCs are composed of the α/β heterodimer and antigenic peptide (αβpeptide). Ii, invariant chain.

αβ dimers, as well as the kinetics of SDS-stable dimer formation. The results from wild-type and 3d mice were indistinguishable (Fig. 2). We did not observe any difference in synthesis and maturation of class I MHC molecules either (unpublished data). We conclude that, at least at this level of analysis, defects in MHC-restricted antigen presentation in 3d mice are unlikely to result from aberrant trafficking of MHC products.

Immunoprecipitation of wild-type UNC93B recovers an ∼130-kD protein that retains Endo H sensitivity

Because wild-type and mutant UNC93B did not show any difference in localization, expression levels, maturation, and stability, the effect of the point mutation may lie in the loss or gain of interaction partners of the UNC93B proteins. Thus far, no interacting proteins have been described for UNC93B.

To identify interacting proteins of UNC93B, we conducted pulse-chase experiments in RAW macrophages stably expressing epitope-tagged wild-type or mutant UNC93B-HA (Fig. 1 A). Cells were lysed after 0, 90, or 180 min of chase in mild detergent (1% digitonin). We used digestion with either Endo H or Peptide:*N*-glycosidase F (PNGase F) to monitor the glycosylation status of UNC93B-HA. As observed for endogenous UNC93B, both wild-type and mutant UNC93B-HA retained Endo H and PNGase F sensitivity throughout the chase period (Fig. 3 A, middle and right).

We noted the presence of a polypeptide of lesser autoradiography intensity, and of a size (∼130 kD) inconsistent with that predicted for UNC93B itself. This polypeptide, too, retained full Endo H sensitivity. The presence of this additional polypeptide was observed only for wild-type, but not for mutant, UNC93B, even though the mutant protein was expressed at levels comparable to that of wild-type UNC93B, as assessed by both immunoblotting (not depicted) and immunoprecipitation on extracts of RAW macrophages stably expressing the relevant constructs (Fig. 1 B and Fig. 3 A). The ability to recruit the ∼130-kD polypeptide, thus correlates with the functional properties of UNC93B. We also observed that an ∼130-kD, Endo H–sensitive polypeptide was coimmunoprecipitated with wild-type, but not with mutant, UNC93B in A20 B cells (Fig. 6 D and not depicted). In A20 B cells, we detected an additional polypeptide of ∼150 kD that had characteristics similar to that of the ∼130-kD polypeptide, in that it was also Endo H–sensitive and was coimmunoprecipitated only with wild-type UNC93B (Fig. 6 D and not depicted).

Large-scale immunoprecipitation of UNC93B identifies TLR3, 7, 9, and 13 as interacting proteins of wild-type, but not of mutant, UNC93B

To identify UNC93B-associated polypeptides, we prepared large-scale cell cultures of RAW macrophages stably expressing

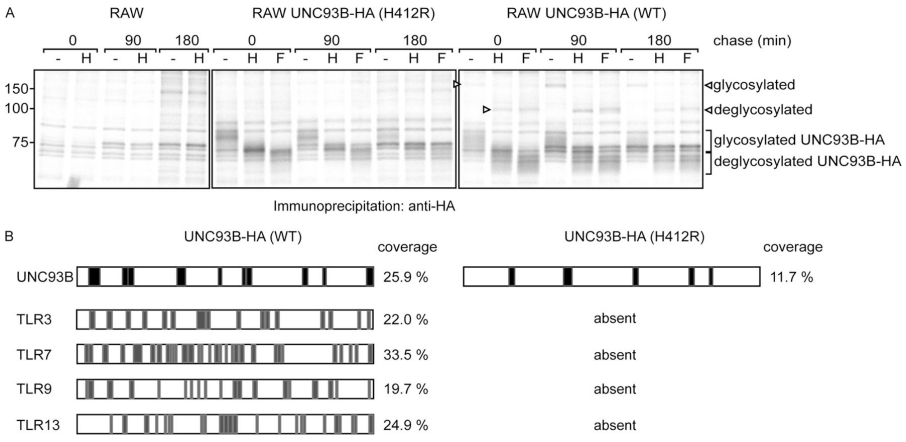

Figure 3. **TLR3, 7, 9, and 13 bind to wild-type, but not mutant, UNC93B.** (A) RAW macrophages (left) or RAW cells stably transduced with either mutant (middle) or wild-type (right) UNC93B-HA were labeled with [^{35}S]methionine/cysteine for 30 min. Cells were lysed in 1% digitonin lysis buffer after chase periods of 0, 90, or 180 min, and UNC93B-HA was immunoprecipitated with an anti-HA antibody. The samples were incubated with Endo H (H) or PNGase F (F) and resolved by SDS-PAGE. The polypeptide (∼130 kD in its glycosylated form; ∼100 kD in its deglycosylated form) that coimmunoprecipitated with wild-type UNC93B is indicated with arrowheads. (B) 4 billion RAW cells expressing wild-type (WT) or mutant (H412R) UNC93B-HA were lysed in 1% digitonin buffer and UNC93B-HA proteins were immunoprecipitated with an anti-HA antibody. After immunoprecipitation, UNC93B and UNC93B-associated proteins were released by incubation with TEV protease, resolved by SDS-PAGE, and visualized by silver staining. Polypeptides were excised from the gel and analyzed by LC/MS/MS after trypsin digestion. Peptides for UNC93B (black) were recovered in both samples, whereas peptides corresponding to sequences of TLR3, 7, 9, and 13 (gray) were identified only in the sample containing wild-type UNC93B. Peptide sequences identified by MS for UNC93B and TLRs are given in Tables S1 and S2, respectively. Tables S1 and S2 are available at http://www.jcb.org/cgi/content/full/jcb.200612056/DC1.

either wild-type or mutant UNC93B-HA and conducted a preparative immunoprecipitation of the tagged UNC93B proteins by retrieval via the HA epitope tag (Fig. 1 A). Bound materials were released by digestion with TEV protease. After resolution of eluted polypeptides by SDS-PAGE and visualization by silver staining, we excised polypeptides unique to wild-type UNC93B-bound material, as well as polypeptides common to both wild-type and mutant UNC93B samples, and determined their identity by MS (Fig. 3 B and Tables S1 and S2, available at http://www.jcb.org/cgi/content/full/jcb.200612056/DC1).

As expected, peptides for UNC93B were identified from both wild-type and mutant UNC93B samples with good sequence coverage, at 25.9% (12 peptides) and 11.7% (6 peptides), respectively (Fig. 3 B and Table S1). Among the polypeptides coimmunoprecipitated only with wild-type UNC93B, we identified TLR3, 7, 9, and 13 with extensive sequence coverage over the entire length of the proteins (TLR3: 22.0%, 17 peptides; TLR7: 33.5%, 35 peptides; TLR9: 19.7%, 20 peptides; TLR13: 24.9%, 26 peptides; Fig. 3 B and Table S2). The same experimental approach was adapted to identify UNC93B-interacting proteins in A20 B cells. Again, we identified multiple peptides corresponding to TLR7 and 9 from the sample for wild-type UNC93B, but none from the sample for mutant UNC93B (unpublished data). We did not recover any peptides of TLR3, 7, 9, or 13 with mutant UNC93B, or any peptide that corresponded to TLR4 or other TLRs with either wild-type or mutant UNC93B in RAW macrophages or A20 B cells. We also carefully examined the proteomics data for the presence of TLR adaptors or signaling molecules implicated in TLR signal transduction pathways. Peptides derived from MyD88, TRIF, or IRAK were not detected, even when MS datasets were interrogated specifically for their presence.

By coimmunoprecipitation and MS, we have thus identified TLR3, 7, 9, and 13 as interacting partners for wild-type UNC93B, and we did not retrieve these TLRs with mutant UNC93B. This suggests that the H412R mutation within the transmembrane domain of UNC93B disrupts interaction between UNC93B and TLRs, and thus abolishes TLR signaling.

Wild-type UNC93B interacts with TLR3 and 9, but not with TLR4

To confirm the interaction between wild-type UNC93B and TLRs, and the failure of mutant UNC93B to associate with TLRs, we generated myc-tagged TLR3, 4, and 9 fusion constructs and coexpressed them together with wild-type and mutant UNC93B-HA in HEK 293-T cells. Cells were lysed under mild conditions and subjected to immunoprecipitation with an anti-myc antibody. The presence of UNC93B in the myc immunoprecipitates was detected by immunoblot analysis with an anti-HA antibody (Fig. 4, top). Wild-type UNC93B interacts with TLR3 and 9, but not with TLR4, confirming our observations made by large-scale coimmunoprecipitation and MS (Fig. 3 B). Mutant UNC93B failed to interact with TLR3, 4, and 9, mirroring our earlier results. Total lysates were analyzed for expression levels of wild-type and mutant UNC93B by immunoblotting with an anti-HA antibody to confirm comparable expression levels (Fig. 4, bottom).

TLR3 and 9 interact with wild-type UNC93B via their transmembrane regions

All TLRs consist of an extracellular domain with a series of leucine-rich repeats, a transmembrane domain, and a cytosolic domain, which contains the conserved Toll-interleukin 1 receptor (TIR) domain. To address which region of the TLRs mediates binding to the UNC93B protein, we generated myc-tagged versions of chimeric TLRs (schematically depicted in Fig. 5 A). Because TLR4 failed to bind to UNC93B, we exchanged the transmembrane regions of TLR3 and 9 with the transmembrane region of TLR4 (TLR3-4-3 and TLR9-4-9), and the transmembrane region of TLR4 was swapped for the transmembrane regions of TLR3 or 9 (TLR4-3-4 and TLR4–9-4). These myc-tagged TLR chimeras and myc-tagged wild-type TLR3, 4, and 9 were coexpressed with wild-type UNC93B-HA. Cells were then metabolically labeled with [^{35}S]methionine/cysteine and lysed under mild conditions. From these lysates, we performed immunoprecipitations with an antibody to either the myc or the HA epitope. The immunoprecipitation with the anti-myc antibody shows the expression levels of the wild-type and chimeric TLR proteins (Fig. 5 B, middle). By immunoprecipitating UNC93B via the HA tag and subsequent reimmunoprecipitation with TLR-specific antibodies, we recovered TLR3 and 9, but not TLR4 (Fig. 5 B, top), confirming our earlier observations (Fig. 3 B and Fig. 4). The chimeric TLRs containing the transmembrane domain of TLR4 (TLR3-4-3 and TLR9-4-9) failed to bind to UNC93B, whereas the TLR4 chimeras containing either the transmembrane region of TLR3 or 9 (TLR4-3-4 or TLR4-9-4) were readily recovered with UNC93B (Fig. 5 B, top). Recovery of UNC93B-HA is shown in Fig. 5 B (bottom). These results establish that TLR3 and 9 interact with the wild-type UNC93B protein via their respective transmembrane regions.

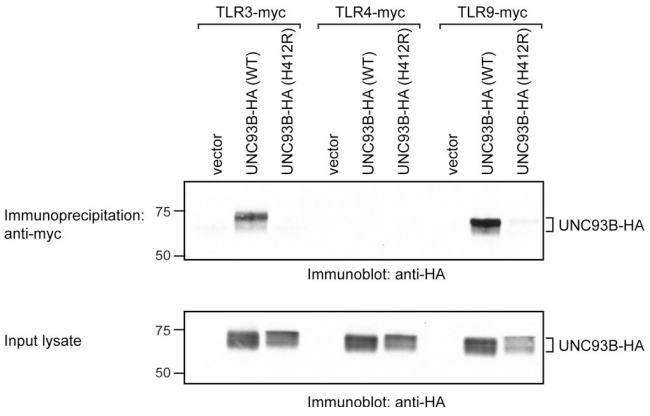

Figure 4. **Wild-type UNC93B associates with TLR3 and 9, but not with TLR4.** HEK 293-T cells were cotransfected with empty vector or expression constructs for wild-type or mutant UNC93B-HA along with expression constructs for myc-tagged TLR3, 4, or 9 (Fig. 5 A). Cells were lysed with 1% digitonin lysis buffer and TLRs were immunoprecipitated with an anti-myc antibody. Samples were resolved by SDS-PAGE, and UNC93B proteins were detected by immunoblotting using an anti-HA antibody (top). Wild-type UNC93B was recovered by immunoprecipitation of TLR3 and 9, whereas the mutant UNC93B (H412R) did not coimmunoprecipitate with any of TLRs. Input lysates were analyzed by SDS-PAGE for expression levels of wild-type and mutant UNC93B-HA with an anti-HA antibody (bottom).

Endogenous wild-type UNC93B and TLR7 associate in BM-DCs

To extend our observations from transduced cells to primary cells, we next analyzed the interactions of UNC93B with TLRs in BM-DCs obtained from wild-type (C57BL/6) and 3d mutant mice. Immunoprecipitation was performed with rabbit anti–UNC-C serum. We recovered considerable quantities of endogenous UNC93B from both wild-type and mutant dendritic cells (Fig. 6 A), confirming the earlier observation that the 3d mutation does not compromise stability or steady-state levels of the UNC93B protein. As seen for RAW cells transfected with epitope-tagged UNC93B, we observed the presence of several coimmunoprecipitating polypeptides in the size range of TLRs in wild-type, but not in mutant, UNC93B immunoprecipitates (Fig. 6 A, left, and Fig. 1 D). The identity of one of the interacting proteins was revealed by denaturation of the primary anti–UNC-C immunoprecipitates, followed by reimmunoprecipitation with an anti-TLR7 antibody. In addition, we used dendritic cells obtained from TLR7-deficient mice as further evidence for the specificity of the anti-TLR7 antibody used. Wild-type UNC93B immunoprecipitates contain TLR7, as seen from the reimmunoprecipitation experiment with the anti-TLR7 antibody (Fig. 6 A, middle). As expected, no TLR7 is found in association with wild-type UNC93B obtained from TLR7-deficient dendritic cells. In dendritic cells obtained from 3d mice, we did not observe coimmunoprecipitation of TLR7 and UNC93B. In addition, the additional polypeptides within the size range of TLRs that were coimmunoprecipitated with wild-type UNC93B are absent from the 3d samples, whereas they are still present in the sample from TLR7-deficient mice. Similar results were obtained when we analyzed interactions between UNC93B and TLRs in splenocytes from wild-type, 3d, TLR7$^{-/-}$, and TLR9$^{-/-}$ mice. Again, TLR7 and TLR9 were coimmunoprecipitated only with wild-type, but not with mutant, UNC93B (Fig. S2, available at http://www.jcb.org/cgi/content/full/jcb.200612056/DC1).

The inability of the mutant UNC93B protein to interact with TLRs might be caused by reduced expression of TLRs in cells from 3d mice. The inability of the 3d mice to signal via TLRs could therefore be the consequence of destabilization of TLRs, if UNC93B would serve a chaperone function. However, this is clearly not the case because we recovered equivalent amounts of TLR7 by direct immunoprecipitation from both wild-type and the 3d dendritic cell lysates using the TLR7 antibody (Fig. 6 B).

In addition, we confirmed the interaction between UNC93B and TLR7 by first immunoprecipitating TLR7 and, subsequently, reimmunoprecipitating UNC93B from the denatured TLR7 immunoprecipitates. Wild-type, but not mutant, UNC93B was recovered by immunoprecipitation of TLR7 (Fig. 6 C).

In summary, we confirmed the physical interaction of UNC93B with TLRs in primary cells and show that the mutant UNC93B protein no longer engages in such complex formation. Our earlier results obtained with the use of epitope-tagged versions of UNC93B are thus valid for endogenous proteins in primary dendritic cells and splenocytes of the appropriate genetic backgrounds.

Activation of TLRs does not affect the interaction between UNC93B and TLRs

To determine whether activation of TLRs with their respective agonists regulates the interaction with UNC93B, we stimulated

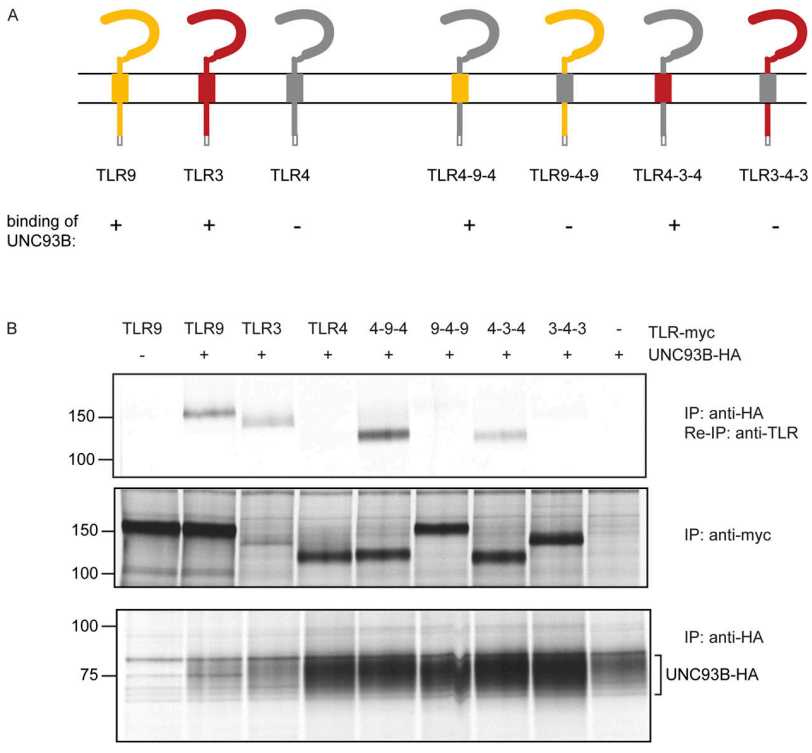

Figure 5. **TLR3 and 9 interact with UNC93B via their transmembrane segments.** (A) Schematic presentation of myc-tagged TLR expression constructs used in this study. The myc-tag was fused to the C terminus of the TLRs, and it is indicated as a white rectangle. The TLR chimeras were generated such that the transmembrane segments were exchanged between TLR3, 4, and 9 to yield TLR3 and 9 with the transmembrane segment of TLR4 (TLR3-4-3 and TLR9-4-9), and TLR4 with the transmembrane segment of either TLR3 (TLR4-3-4) or TLR9 (TLR4-9-4). Binding capabilities of wild-type UNC93B to TLRs as shown in this study are indicated (–, no binding; +, binding). (B) HEK 293-T cells were cotransfected with an empty vector (–) or an expression construct for wild-type UNC93B-HA together with myc-tagged TLR3, 4 or 9 or the myc-tagged TLR chimeras TLR4-9-4, 9-4-9, 4-3-4, 3-4-3. Cells were metabolically labeled for 4 h with [^{35}S]methionine/cysteine and lysed in 1% digitonin lysis buffer. One fifth of the lysate was subjected to immunoprecipitation with an anti-myc antibody to assess the expression of the TLR constructs (middle). The rest of the lysate was subjected to immunoprecipitation with an anti-HA antibody and one tenth of the resulting UNC93B-HA immunoprecipitates was directly resolved by SDS-PAGE to show UNC93B-HA expression levels (bottom). The remaining UNC93B-HA immunoprecipitates were subjected to denaturation, and reimmunoprecipitations were performed with TLR-specific antibodies (anti-TLR3 for TLR3, TLR3-4-3, untransfected; anti-TLR4 for TLR4, TLR4-3-4, TLR4-9-4; anti-TLR9 for TLR9, TLR9-4-9) and resolved by SDS-PAGE (top). TLR3 and 9 were recovered by reimmunoprecipitation from UNC93B-HA immunoprecipitates, as well as the TLR chimeras TLR4-3-4 and TLR4-9-4, but not TLR4 and chimeras TLR9-4-9 and TLR3-4-3.

A20 B cells that stably express wild-type or mutant UNC93B-HA with TLR7 and 9 agonists; imiquimod or gardiquimod for TLR7 and CpG DNA for TLR9. After metabolically labeling cells with [^{35}S]methionine/cysteine, cell lysates were subjected to immunoprecipitation with an anti-HA antibody to retrieve UNC93B. No substantial changes in the levels of coimmunoprecipitated TLR polypeptides were observed after TLR activation when compared with unstimulated cells, nor did we see additional interacting proteins for agonist-exposed cells (Fig. 6 D). Similarly, stimulation with the TLR agonists did not alter the interaction between endogenous UNC93B and TLRs in splenocytes and dendritic cells from wild-type mice (unpublished data).

Discussion

TLRs are involved in the perception and processing of signals delivered by viral and microbial products and coordinate both innate and adaptive immunity. Mutations in UNC93B cause signaling defects for multiple TLRs and raise the question of the mechanism of its involvement in TLR signaling.

By expression of epitope-tagged UNC93B and production of polyclonal antibodies that recognize endogenous UNC93B, we characterized UNC93B as a glycosylated ER-resident protein. The mutant UNC93B (H412R) protein exhibits distinct migration patterns in SDS-PAGE compared with wild-type UNC93B. Its behavior suggests a role for His412 in the intramolecular organization of UNC93B, as denaturation of polytopic membrane proteins using SDS without boiling is likely to preserve at least some features of secondary structure. Nonetheless, the 3d mutation (H412R) in UNC93B does not compromise biosynthesis and maturation of the mutant protein, and both wild-type and mutant proteins are equally stable.

To study the role of UNC93B in TLR signaling, we identified UNC93B binding proteins using a large-scale preparative immunoprecipitation in conjunction with MS. We found that wild-type, but not mutant, UNC93B interacts with TLR3, 7, 9, and 13. We also found that TLR4 does not interact with either wild-type or mutant UNC93B. The number of peptides and the extent of sequence coverage of TLRs identified by MS suggest that these TLRs are well-represented among proteins that bind to UNC93B. The interaction between wild-type UNC93B and

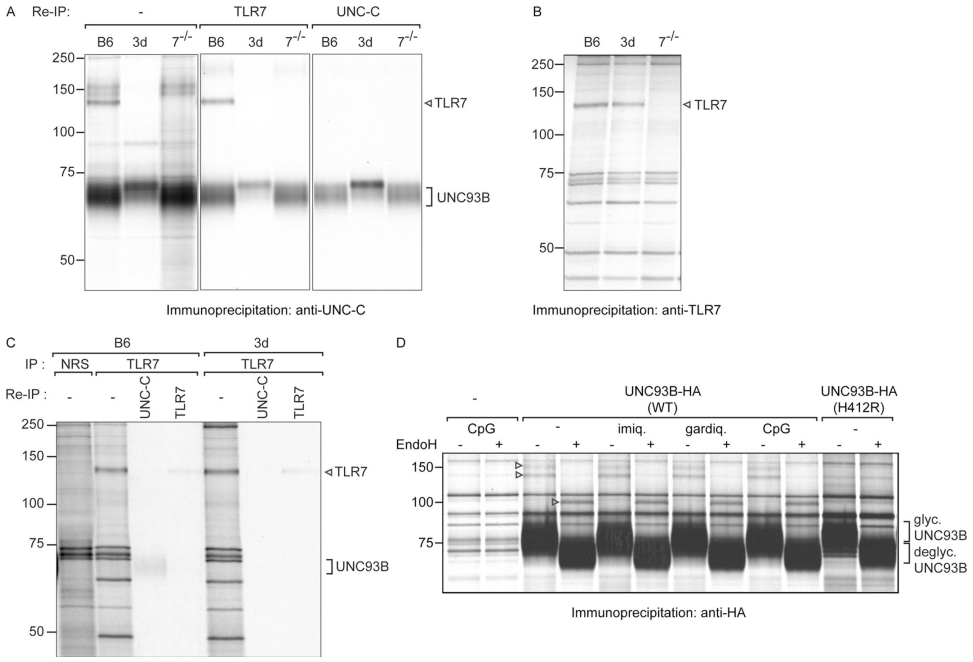

Figure 6. **Endogenous UNC93B and TLR7 associate in BM-DCs from wild-type, but not from UNC93B mutant mice.** (A–C) Day 5 cultures of BM-DCs prepared from wild-type (C57BL/6, B6), UNC93B mutant (3d) or TLR7$^{-/-}$ mice were metabolically labeled for 4 h with [^{35}S]methionine/cysteine and lysed in 1% digitonin lysis buffer. (A) The first immunoprecipitation was performed with the purified anti–UNC-C antibody (left). After mild denaturation of the initial immunoprecipitates, reimmunoprecipitations were performed with either an anti-TLR7 antibody (middle) or the anti–UNC-C antiserum (right). TLR7 was recovered with wild-type, but not with mutant UNC93B. Expression levels of wild-type and mutant UNC93B were comparable. (B) TLR7 expression levels in wild-type (B6), UNC93B mutant (3d), and TLR7 knockout (TLR7$^{-/-}$) mice were analyzed by direct immunoprecipitation of TLR7 with the TLR7 antibody. Endogenous TLR7 is present at equal levels in both wild-type and UNC93B mutant 3d mice, but absent in TLR7 knockout mice. (C) TLR7 was immunoprecipitated with the TLR7 antibody from digitonin lysates of BM-DCs from wild-type (B6) or UNC93B mutant (3d) mice. Immunoprecipitation with normal rabbit serum (NRS) served as a control for TLR7 immunoprecipitation. Reimmunoprecipitations with anti–UNC-C or anti-TLR7 antibodies were performed after mild denaturation of the initial TLR7 immunoprecipitates and resolved by SDS-PAGE. UNC93B was coimmunoprecipated with TLR7 in BM-DC lysates from wild-type, but not from UNC93B mutant, mice. Recovery of TLR7 from BM-DCs of both wild-type and mutant mice by immunoprecipitation and reimmunoprecipitation was equal. (D) Nontransduced A20 B cells (–) or A20 B cells stably transduced with wild-type (WT) or mutant UNC93B-HA (H412R) were metabolically labeled for 4 h with [^{35}S]methionine/cysteine (pulse) and stimulated with TLR7 agonists imiquimod (10 μM) or gardiquimod (1 μM) or the TLR9 agonist CpG DNA (1 μM) for 1 h during the final hour of the pulse. Cells were lysed in 1% digitonin lysis buffer, and immunoprecipitations were performed with an anti-HA antibody. Samples were not treated (–) or digested with Endo H (+) and resolved by SDS-PAGE. The polypeptides that associate only with wild-type UNC93B and have characteristics of TLRs are indicated by arrowheads. Interaction of these polypeptides with wild-type UNC93B was not considerably changed in stimulated cells compared with nonstimulated cells.

TLRs (TLR3, 7, and 9) was confirmed by additional biochemical analyses in cell lines and primary cells. The interactions between wild-type UNC93B and TLRs (TLR3, 7, 9, and 13) and the absence of interaction between UNC93B and TLR4 correlate well with the phenotype of the 3d mice, which show specific defects in signaling via TLR3, 7, and 9, but not TLR4 (Tabeta et al., 2006). In addition, we demonstrated the expression of TLR13 in a macrophage cell line. TLR13 was identified by homology search of TIR domain-containing proteins in mouse ESTs, but no function has been assigned to it (Tabeta et al., 2004). It will be interesting to see whether signaling via this less well-characterized TLR is also affected in 3d mice, as we predict it will be.

Many studies demonstrate that TLR3, 7, and 9 are localized intracellularly (Ahmad-Nejad et al., 2002; Matsumoto et al., 2003; Latz et al., 2004; Leifer et al., 2004; Nishiya and DeFranco, 2004). TLR9 resides in the ER before stimulation and reaches lysosomes only upon activation (Latz et al., 2004; Leifer et al., 2004). The ER localization of TLR9 is consistent with our data showing that ER-localized UNC93B physically interacts with TLR9. UNC93B retains full Endo H sensitivity, which is also consistent with previous observations that TLR9 remains sensitive to Endo H digestion even after activation (Latz et al., 2004; Leifer et al., 2004). The transmembrane domains of TLR7 and 9 and the cytosolic linker region between the transmembrane domain and TIR domain of TLR3 determine the intracellular localization for these TLRs (Funami et al., 2004; Nishiya et al., 2005; Barton et al., 2006; Kajita et al., 2006). By using chimeric TLRs, we show that the transmembrane domains of TLR3 and 9 are responsible for binding to UNC93B. When the transmembrane domain of TLR4 is substituted for the transmembrane domain of either TLR3 or 9, the chimeric TLR4 proteins acquire the ability to interact with UNC93B. In contrast, TLR3 and 9 chimeras equipped with the TLR4 transmembrane domain no longer bind to UNC93B.

The strength of interaction between UNC93B with its client TLRs is robust, as judged from the quantities of TLRs detected by direct immunoprecipitation and that were found in association with UNC93B. This result suggests that a considerable fraction, if not the majority of TLR3, 7, and 9, may be associated with UNC93B. The results of pulse-chase analyses are likewise consistent with stable association of UNC93B with TLRs. These observations raise the question as to the function of UNC93B. How does UNC93B participate in TLR signaling? One possibility is that UNC93B acts as an ER chaperone for TLR3, 7, 9, and 13. However, given the observation that the transmembrane segment of a TLR is sufficient to dictate interactions with UNC93B, and that interaction between UNC93B and TLRs is not transient, but is maintained for a prolonged period of time, we consider a classical chaperone function for UNC93B as less likely. Chaperone–client interactions are usually transient, and for glycoproteins they involve mostly the luminal/extracellular domains. Moreover, the expression level of TLR7 is not altered in BM-DCs from 3d mice compared with wild-type mice, arguing against the possibility that UNC93B would act by stabilization of its client TLRs. Instead, by analogy with the function of another ER-resident protein gp96, which is essential for TLR4/MD-2 complex assembly (Randow and Seed, 2001), UNC93B may be involved in the assembly of intracellular TLRs with thus far unidentified proteins that are essential for either ligand recognition or signal transduction. Alternatively, UNC93B may play a role in retaining the client TLRs in the ER until they are ready to traffic to endosomes. TLR9 resides in the ER until activated (Latz et al., 2004; Leifer et al., 2004). Although there is no consensus on exactly where TLR3 localizes, it seems that a large proportion of TLR3 co-localizes with TLR9 at steady-state (Nishiya et al., 2005; Kajita et al., 2006). The previously demonstrated essential role of the transmembrane domain of TLR9 for ER localization and identification of the TLR9 transmembrane domain as the UNC93B-binding determinant in this study supports the role of UNC93B in ER retention of TLRs. This suggestion is at variance with the report by Tabeta et al. (2006), which reports no discernible changes in TLR9 localization in 3d mice.

MD-2 directly interacts with TLR4 and plays an important role in the recognition of LPS (Shimazu et al., 1999). In addition, MD-2 was suggested to contribute to the surface localization of TLR4 (Nagai et al., 2002). In MD-2–deficient mouse embryonic fibroblasts, TLR4 is retained in the Golgi apparatus. Although MD-2–bound TLR4 is directed to the cell surface constitutively, UNC93B may play a role in the transport of its client TLRs to endosomes in a stimulation-dependent manner. Trafficking of TLR9 from ER to lysosomal compartments after uptake of CpG in dendritic cells may, thus, depend on the interaction between UNC93B and TLR9. Because both UNC93B and TLRs retain full Endo H sensitivity; even after TLR stimulation they may travel to endosomes via an unconventional anterograde route that does not involve the Golgi apparatus, should the UNC93B–TLR complex, indeed, traffic together to endosomes. High-resolution microscopy studies on localization of TLRs after proper stimulation may provide new insights into the possible role of UNC93B in TLR trafficking.

Upon activation, many receptors recruit adaptor molecules onto which various downstream signaling molecules assemble for efficient and coordinated signal transduction. For some receptors, a scaffolding protein that constitutively binds the receptor provides a platform to which signaling molecules are recruited. UNC93B may serve as such a scaffold for TLR signaling or be an integral part of a signaling unit. The exposed loops and N and C termini of UNC93B could serve to organize and orient the other components of the TLR signaling complex. The stably maintained interactions between UNC93B and TLRs, even after activation of TLRs, support this hypothesis. Our initial large-scale immunoprecipitation of UNC93B, and the subsequent MS analysis, did not identify any prominent signaling molecules of the TLR signaling pathways. Furthermore, experiments designed to directly test the association of UNC93B with MyD88 did not yield any evidence for such interactions (unpublished data). However, it will still be interesting to see what additional proteins bind to UNC93B after stimulating cells with TLR agonists.

The TLR signaling defects in cells from 3d mice are mimicked by pretreating wild-type cells with chloroquine or bafilomycin, which are agents that inhibit endosome acidification, but

the 3d mutation does not affect the pH of different intracellular organelles (Tabeta et al., 2006). Therefore, UNC93B does not seem to be directly involved in endosome acidification. Human UNC93B protein contains a region of weak homology to the bacterial ABC-2–type transporters (Kashuba et al., 2002). In addition, homology searches of the conserved domains (rps-blast; National Center for Biotechnology Information BLAST) identified a second domain (residues 101 and 185 of UNC93B) with similarity to a bacterial transporter (MelB, E-value of 0.03). Even though sequence homology is weak in both cases, these observations raise the possibility that UNC93B could have a yet to be identified transporter function. The ectodomain of the microbial nucleotide-sensing TLRs (TLR3, 7, and 9) faces the lumen of the ER and endosomes. It is likely that viral DNAs and RNAs need to gain access to such an environment for signaling through their cognate TLRs. Therefore, UNC93B may participate in such processes and position the TLRs for efficient recognition of their agonists.

The exact identities of intracellular compartments where the nucleotide-sensing TLRs receive stimulating signals from microbial DNAs and RNAs are still an open question. Studies using chemical inhibitors that prevent endosome acidification have proposed the endosomes as the location where intracellular TLR9 initiates signaling and potentially recognizes ligands (Ahmad-Nejad et al., 2002; Barton et al., 2006). However, upon addition of CpG DNA, even in MyD88-deficient dendritic cells, TLR9 travels normally from the ER to endosomes, where internalized CpG accumulates (Latz et al., 2004). If translocation of TLR9 to endosomes is indeed a signal-mediated event, these data imply that either TLR9 receives a stimulatory signal of CpG DNA before reaching the endosomes, perhaps in the ER, or there is an additional molecule that senses CpG and triggers translocation of TLR9 in a MyD88-independent manner. The possibility that TLR9 may sense CpG in the ER or ER-derived structures deserves consideration. Pathways for retrograde transport of microbial products to the ER include delivery of the intact pathogen itself, as exemplified by SV40 and polyoma virus (Spooner et al., 2006). Bacterial toxins, such as cholera toxin and shiga toxin, likewise travel from the cell surface to the ER, from which they are discharged into the cytoplasm to intoxicate the cells exposed to the toxin (Spooner et al., 2006). In addition, it has been claimed that exogenously added soluble proteins can access the ER lumen in dendritic cells (Ackerman et al., 2005). Therefore, the delivery of TLR ligands to the ER itself is certainly a possibility. Potentially, UNC93B could play a role in the perception of ER-delivered microbial nucleotides in concert with the intracellular TLRs.

The reported phenotype of 3d mice includes defects in cross-presentation and MHC class II–mediated antigen presentation. Despite the defects in presentation of exogenous antigens, the subcellular distribution of MHC class I and II proteins was not affected (Tabeta et al., 2006). Consistent with this observation, biosynthesis, maturation, and assembly of MHC class I and II molecules were identical in BM-DCs from wild-type and 3d mice. Although it remains unclear how UNC93B participates in antigen presentation, it is worth noting that a series of recent, controversial, observations suggests the involvement of the ER or ER-derived intracellular compartments in cross-presentation of exogenous antigens (Ackerman et al., 2005, 2006; Imai et al., 2005). The role of UNC93B in cross-presentation deserves to be further explored in this context.

In summary, we demonstrate that wild-type, but not mutant, UNC93B (H412R) physically interacts with TLR3, 7, 9, and 13. The established interaction between UNC93B and TLRs sheds new light on the 3d mutation and its TLR signaling-defective phenotype. The prominent ER localization of UNC93B, and of the TLRs to which it binds, raises the intriguing possibility that the ER itself may serve as a compartment from which TLR signaling is initiated.

Materials and methods

Cell lines

Murine RAW 264.7 macrophages (TIB-71; American Type Culture Collection [ATCC]) and human embryonic kidney (HEK) cells 293-T (CRL-11268; ATCC) were maintained in DME containing 10% heat-inactivated fetal calf serum (HIFS) and penicillin/streptomycin. Murine A20 B cells (TIB-208; ATCC) were maintained in RPMI 1640 medium supplemented with 10% IFS and penicillin/streptomycin. 293-T cells were transfected with FuGene-6 (Roche) according to the manufacturer's instructions.

Animals

C57BL/6 wild-type mice were purchased from Taconic. The TLR7$^{-/-}$ (Hemmi et al., 2002) and TLR9$^{-/-}$ (Hemmi et al., 2002) mice were obtained from A. Marshak-Rothstein (Boston University, Boston, MA). All animals were maintained under specific pathogen-free conditions, and experiments were performed in accordance with institutional, state, and federal guidelines.

Antibodies and reagents

Antibodies against mouse UNC93B were generated against the N-terminal (anti–UNC-N; aa 1–59) and the C-terminal (anti–UNC-C; aa 515–598) region. Three peptides were chosen for each region with an Antigen Profiler (Open Biosystems) and synthesized with a cysteine residue added to the N terminus by the Massachussetts Institute of Technology Center for Cancer Research Biopolymers Laboratory. N-terminal UNC93B peptides were as follows: 1N, C-DRHGVPDGPEAPLDE; 2N, C-PDGPEAPLDELVGAY; and 3N, C-GAYPNYNEEEEERRYYRRK. C-terminal UNC93B peptides were as follows: 1C, C-LQQGLVPRQPRIPKP; 2C, C-RYLEEDNSDESDMEG; and 3C, CPYEQALGGDGPEEQ. Peptides were analyzed by HPLC and MS for purity and coupled individually to keyhole-limpet hemocyanin (Pierce Chemical Co.) via the cysteine residue using sulfosuccinimidyl 4-[*N*-maleimidomethyl]-cyclohexane-1-carboxylate (sulfo-SMCC; Pierce Chemical Co.) according to the manufacturer's recommendations. After coupling, the three peptides (1–3N or 1–3C) were mixed, and antisera were raised in rabbits by an outside vendor (Covance). The anti–UNC-C polyclonal serum was affinity purified using the three peptides of the C-terminal region (1C, 2C, and 3C) that are coupled to the resin using the Sulfo Link kit (Pierce Chemical Co.). The affinity-purified anti–UNC-C antibody was used for immunoprecipitations and immunoblotting. The TLR7 antibody and the TLR4 antibody (M16) were obtained from Imgenex and Santa Cruz Biotechnology, respectively. Rabbit polyclonal TLR3 and 9 antibodies are raised against peptide sequences in the C-terminal domain of the respective protein. The Flag antibody (M2; mouse monoclonal) was purchased from Sigma-Aldrich. The anti-HA affinity matrix (3F10, rat monoclonal) was purchased from Roche. The anti-HA 12CA5 antibody (mouse monoclonal) was produced in our laboratory from hybridoma cells. The anti-myc (9E10, mouse monoclonal) antibody was purchased from Invitrogen. The MHC class II antibody is a hamster monoclonal antibody (clone N22). Imiquimod (R837) and gardiquimod were purchased from Invivogen, CpG DNA (1826-CpG) was obtained from TIB Molbiol, and LPS (*Escherichia coli* 026:B6) was purchased from Sigma-Aldrich.

DNA cloning

Murine UNC93B (BC018388) was C-terminally fused with the Flag tag, followed by the TEV protease cleavage site (ENLYFQG) and the HA tag (UNC93B-HA, WT; see scheme in Fig. 1 A). The point mutant UNC93B (H412R) was generated by sequential PCR with primers carrying the point

mutation CAC (His) to CGC (Arg) and C-terminally fused with the Flag tag, followed by the TEV protease cleavage site and the HA tag (UNC93B-HA, H412R). UNC93B-HA WT and H412R were cloned into the retroviral vector pMSCVneo (Clontech Laboratories, Inc.), and stable cell lines in RAW or A20 B cells were established by retroviral transduction and selection with geneticin (see the following section).

The TLR9 cDNA in pcDNA3.1 was provided by S. Bauer (Institut für Medizinische Mikrobiologie, München, Germany; Bauer et al., 2001). C-terminally myc-tagged murine TLR3 (BC099937), TLR4 (BC029856), and TLR9 (AF348140) were generated by PCR and cloned into the pMSCVpuro (Clontech Laboratories, Inc.) or pcDNA3.1 vector (Invitrogen). The TLR chimeras were constructed by PCR "sewing" with cDNA corresponding to the following amino acids of the TLRs: TLR4-3-4, 1–625 of TLR4, 698–726 of TLR3, and 660–835 of TLR4; TLR3-4-3, 1–697 of TLR3, 626–659 of TLR4, and 727–905 of TLR3; TLR4-9-4, 1–625 of TLR4, 811–839 of TLR9, and 660–835 TLR4; and TLR9-4-9, 1–810 of TLR9, 626–659 of TLR4, 840–1032 of TLR9. All TLR chimeric constructs were C-terminally myc-tagged and cloned into the pMSCVpuro vector. The sequence of all constructs generated by PCR was verified.

Retroviral transduction

HEK 293-T cells were transfected with plasmids encoding VSV-G or Env, Gag-Pol, and pMSCV-UNC93B-HA (WT) or pMSCV-UNC93B-HA (H412R). 24 h after transfection, medium containing viral particles was collected, filtered through a 0.45-μm membrane, and added to RAW macrophages (VSV-G) or A20 B cells (Env) cells. Cells were spun for 2 h at 2,000 rpm, medium was changed, and cells were selected with 750 μg/ml geneticin (Invitrogen) 2 d after transduction.

Preparation of BM-DCs

BM-DCs were prepared from C57BL/6, UNC93B mutant (3d), TLR7-deficient ($TLR7^{-/-}$), or TLR9-deficient ($TLR9^{-/-}$) mice, as previously described (Maehr et al., 2005).

TNF ELISA assay

BM-DCs derived from wild-type (C57BL/6), UNC93B mutant (3d), TLR7, or TLR9 knockout mice were stimulated for 4 h with increasing concentrations of the TLR agonists LPS (TLR4), imiquimod (TLR7), or CpG DNA (TLR9). The conditioned medium was collected and analyzed by ELISA using the hamster anti–mouse/rat TNF antibody (BD Biosciences) as a capture antibody and a rabbit anti–mouse biotin-labeled secondary antibody (BD Biosciences).

Stimulation with TLR agonists

A20 B cells either not transduced or stably transduced with UNC93B-HA WT or H412R were metabolically labeled with [^{35}S]methionine/cysteine for 4 h (pulse). TLR agonists were added to the cells for the final hour of the pulse at the following concentrations: 10 μM imiquimod, 1 μM gardiquimod, and 1 μM CpG DNA. Cells were lysed in 1% digitonin lysis buffer and immunoprecipitation was performed as indicated in the figure legend.

Pulse-chase, immunoprecipitation, and Endo H/F assay

In brief, cells were starved for methionine and cysteine in Met/Cys-free DME (starvation medium) for 30 min, pulsed for different time periods, as indicated in the figure legends, with [^{35}S]methionine/cysteine (Perkin Elmer) in starvation medium supplemented with dialyzed HIFS, and chased with an excess of nonradioactive amino acids in regular DME for various time periods, as indicated in the figure legends. Cells were lysed in either of the following lysis buffers supplemented with the complete protease inhibitors (Roche), as indicated in the figure legends: RIPA (20 mM Tris-HCl, pH 7.4, 1 mM EDTA, 100 mM NaCl, 1% Triton X-100, 0.5% sodium deoxycholate, and 0.1% SDS) or buffer containing 50 mM Tris-HCl, pH 7.4, 150 mM NaCl, and 5 mM EDTA with either 1% NP-40 or 1% digitonin as detergent. Lysates were equalized for incorporation of radioactive material with ^{35}S counts in the trichloroacetic acid precipitate and immunoprecipitated with the indicated antibodies. Washes were performed with the same buffers used for lysis, except for digitonin lysates/immunoprecipitations, which were washed with 0.1–0.2% digitonin-containing buffer. Reimmunoprecipitations were performed as follows: protein–antibody complexes were dissolved by mild denaturation with 1% SDS and 1% β-mercaptoethanol for 1 h at 37°C. Subsequently, SDS and β-mercaptoethanol were diluted to 0.1% by addition of 1% NP-40 lysis buffer and reimmunoprecipitations were performed with the indicated antibodies. Immunoprecipitates were subjected to 10% SDS–PAGE without heating the samples, and polypeptides were visualized by fluorography. Digestions with Endo H and PNGase F were performed where indicated, in accordance with the manufacturer's instructions (New England BioLabs).

Immunoprecipitations and immunoblotting

In brief, cells were lysed in 1% NP-40, 1% digitonin, or RIPA buffer, and immunoprecipitation was performed with antibodies, as indicated in figure legends. The samples were subjected to 10% SDS–PAGE, transferred to a nitrocellulose membrane, and immunoblotted with the antibodies indicated.

Large-scale affinity purification and MS

The procedure was adapted from Lilley and Ploegh (2004). In brief, 4 billion RAW cells stably expressing UNC93B-HA (WT), UNC93B-HA (H412R), or no exogenous UNC93B protein (control cells) were lysed in 30 ml of ice-cold lysis buffer (1% digitonin, 50 mM Tris-HCl, pH 7.4, 150 mM NaCl, 5 mM EDTA, and complete protease inhibitors [Roche]), with rocking at 4°C for 1 h. The lysate was cleared of cell debris and nuclei by centrifugation at 20,000 *g* for 15 min. UNC93B-HA and associated proteins were retrieved from 150 mg of cleared lysate by immunoprecipitation with 330 μl of compact anti-HA antibody beads. After incubation for 3 h, beads were extensively washed in wash buffer (the same composition as lysis buffer, except with 0.1% digitonin and without protease inhibitors). Bound material was eluted by incubation with 100 U TEV protease (Invitrogen) at 4°C overnight in 200 μl wash buffer. The eluate was exchanged into 20 mM NH_4CO_3, pH 8.0, with 0.1% SDS with the use of Sephadex G-25 resin (GE Healthcare) and concentrated in a Speed Vac (Savant). Reducing SDS loading buffer was added to the sample, and polypeptides were separated by 10% SDS–PAGE and revealed by silver staining. The bands of interest were excised, subjected to trypsinolysis, separated by liquid chromatography, analyzed by MS/MS, and database searched, as previously described (Lilley and Ploegh, 2004).

Online supplemental material

Fig. S1 shows TNF secretion in response to TLR agonists in BM-DCs from wild-type versus UNC93B mutant mice. Fig. S2 shows that TLR7 and 9 coimmunoprecipitate with wild-type UNC93B in splenocytes from wild-type, but not UNC93B mutant, mice. Table S1 shows peptide sequences of UNC93B as identified by LC/MS/MS. Table S2 shows peptide sequences of TLR3, 7, 9, and 13 as identified by LC/MS/MS. The online version of this article is available at http://www.jcb.org/cgi/content/full/jcb.200612056/DC1.

We are very grateful to Dr. Ann Marshak-Rothstein for providing the UNC93B mutant (3d), $TLR7^{-/-}$, and $TLR9^{-/-}$ mice. Dr. Stefan Bauer kindly provided the murine TLR9 cDNA. We thank Drs. Victor Quesada, Marie-Eve Paquet, Howard Hang, and Britta Mueller for helpful discussions and critical reading of the manuscript.

This study was supported by grants from National Institutes of Health (to H.L. Ploegh), the German Research Council (BR 3432/1-1 to M.M. Brinkmann), and the Leukemia & Lymphoma Society (to Y.-M. Kim).

Submitted: 12 December 2006
Accepted: 21 March 2007

References

Ackerman, A.L., C. Kyritsis, R. Tampe, and P. Cresswell. 2005. Access of soluble antigens to the endoplasmic reticulum can explain cross-presentation by dendritic cells. *Nat. Immunol.* 6:107–113.

Ackerman, A.L., A. Giodini, and P. Cresswell. 2006. A role for the endoplasmic reticulum protein retrotranslocation machinery during crosspresentation by dendritic cells. *Immunity*. 25:607–617.

Ahmad-Nejad, P., H. Hacker, M. Rutz, S. Bauer, R.M. Vabulas, and H. Wagner. 2002. Bacterial CpG-DNA and lipopolysaccharides activate Toll-like receptors at distinct cellular compartments. *Eur. J. Immunol.* 32:1958–1968.

Akira, S., K. Takeda, and T. Kaisho. 2001. Toll-like receptors: critical proteins linking innate and acquired immunity. *Nat. Immunol.* 2:675–680.

Alexopoulou, L., A.C. Holt, R. Medzhitov, and R.A. Flavell. 2001. Recognition of double-stranded RNA and activation of NF-kappaB by Toll-like receptor 3. *Nature*. 413:732–738.

Barton, G.M., J.C. Kagan, and R. Medzhitov. 2006. Intracellular localization of Toll-like receptor 9 prevents recognition of self DNA but facilitates access to viral DNA. *Nat. Immunol.* 7:49–56.

Bauer, S., C.J. Kirschning, H. Hacker, V. Redecke, S. Hausmann, S. Akira, H. Wagner, and G.B. Lipford. 2001. Human TLR9 confers responsiveness

to bacterial DNA via species-specific CpG motif recognition. *Proc. Natl. Acad. Sci. USA*. 98:9237–9242.

Beutler, B., Z. Jiang, P. Georgel, K. Crozat, B. Croker, S. Rutschmann, X. Du, and K. Hoebe. 2006. Genetic analysis of host resistance: Toll-like receptor signaling and immunity at large. *Annu. Rev. Immunol.* 24:353–389.

Casrouge, A., S.Y. Zhang, C. Eidenschenk, E. Jouanguy, A. Puel, K. Yang, A. Alcais, C. Picard, N. Mahfoufi, N. Nicolas, et al. 2006. Herpes simplex virus encephalitis in human UNC-93B deficiency. *Science*. 314:308–312.

Curran, A.R., and D.M. Engelman. 2003. Sequence motifs, polar interactions and conformational changes in helical membrane proteins. *Curr. Opin. Struct. Biol.* 13:412–417.

de la Cruz, I.P., J.Z. Levin, C. Cummins, P. Anderson, and H.R. Horvitz. 2003. sup-9, sup-10, and unc-93 may encode components of a two-pore K+ channel that coordinates muscle contraction in *Caenorhabditis elegans*. *J. Neurosci.* 23:9133–9145.

Diebold, S.S., T. Kaisho, H. Hemmi, S. Akira, and C. Reis e Sousa. 2004. Innate antiviral responses by means of TLR7-mediated recognition of single-stranded RNA. *Science*. 303:1529–1531.

Funami, K., M. Matsumoto, H. Oshiumi, T. Akazawa, A. Yamamoto, and T. Seya. 2004. The cytoplasmic 'linker region' in Toll-like receptor 3 controls receptor localization and signaling. *Int. Immunol.* 16:1143–1154.

Greenwald, I.S., and H.R. Horvitz. 1980. unc-93(e1500): a behavioral mutant of *Caenorhabditis elegans* that defines a gene with a wild-type null phenotype. *Genetics*. 96:147–164.

Heil, F., H. Hemmi, H. Hochrein, F. Ampenberger, C. Kirschning, S. Akira, G. Lipford, H. Wagner, and S. Bauer. 2004. Species-specific recognition of single-stranded RNA via toll-like receptor 7 and 8. *Science*. 303:1526–1529.

Hemmi, H., T. Kaisho, O. Takeuchi, S. Sato, H. Sanjo, K. Hoshino, T. Horiuchi, H. Tomizawa, K. Takeda, and S. Akira. 2002. Small anti-viral compounds activate immune cells via the TLR7 MyD88-dependent signaling pathway. *Nat. Immunol.* 3:196–200.

Hemmi, H., O. Takeuchi, T. Kawai, T. Kaisho, S. Sato, H. Sanjo, M. Matsumoto, K. Hoshino, H. Wagner, K. Takeda, and S. Akira. 2000. A Toll-like receptor recognizes bacterial DNA. *Nature*. 408:740–745.

Hoebe, K., X. Du, P. Georgel, E. Janssen, K. Tabeta, S.O. Kim, J. Goode, P. Lin, N. Mann, S. Mudd, et al. 2003. Identification of Lps2 as a key transducer of MyD88-independent TIR signalling. *Nature*. 424:743–748.

Hoshino, K., T. Sugiyama, M. Matsumoto, T. Tanaka, M. Saito, H. Hemmi, O. Ohara, S. Akira, and T. Kaisho. 2006. IkappaB kinase-alpha is critical for interferon-alpha production induced by Toll-like receptors 7 and 9. *Nature*. 440:949–953.

Imai, J., H. Hasegawa, M. Maruya, S. Koyasu, and I. Yahara. 2005. Exogenous antigens are processed through the endoplasmic reticulum-associated degradation (ERAD) in cross-presentation by dendritic cells. *Int. Immunol.* 17:45–53.

Iwasaki, A., and R. Medzhitov. 2004. Toll-like receptor control of the adaptive immune responses. *Nat. Immunol.* 5:987–995.

Janeway, C.A., Jr., and R. Medzhitov. 2002. Innate immune recognition. *Annu. Rev. Immunol.* 20:197–216.

Kajita, E., T. Nishiya, and S. Miwa. 2006. The transmembrane domain directs TLR9 to intracellular compartments that contain TLR3. *Biochem. Biophys. Res. Commun.* 343:578–584.

Kashuba, V.I., A.I. Protopopov, S.M. Kvasha, R.Z. Gizatullin, C. Wahlestedt, L.L. Kisselev, G. Klein, and E.R. Zabarovsky. 2002. hUNC93B1: a novel human gene representing a new gene family and encoding an unc-93-like protein. *Gene*. 283:209–217.

Kawai, T., and S. Akira. 2006. TLR signaling. *Cell Death Differ.* 13:816–825.

Kawai, T., O. Adachi, T. Ogawa, K. Takeda, and S. Akira. 1999. Unresponsiveness of MyD88-deficient mice to endotoxin. *Immunity*. 11:115–122.

Latz, E., A. Schoenemeyer, A. Visintin, K.A. Fitzgerald, B.G. Monks, C.F. Knetter, E. Lien, N.J. Nilsen, T. Espevik, and D.T. Golenbock. 2004. TLR9 signals after translocating from the ER to CpG DNA in the lysosome. *Nat. Immunol.* 5:190–198.

Leifer, C.A., M.N. Kennedy, A. Mazzoni, C. Lee, M.J. Kruhlak, and D.M. Segal. 2004. TLR9 is localized in the endoplasmic reticulum prior to stimulation. *J. Immunol.* 173:1179–1183.

Levin, J.Z., and H.R. Horvitz. 1992. The *Caenorhabditis elegans unc-93* gene encodes a putative transmembrane protein that regulates muscle contraction. *J. Cell Biol.* 117:143–155.

Lilley, B.N., and H.L. Ploegh. 2004. A membrane protein required for dislocation of misfolded proteins from the ER. *Nature*. 429:834–840.

Liu, Y., P. Dodds, G. Emilion, A.J. Mungall, I. Dunham, S. Beck, R.S. Wells, F.M. Charnock, and T.S. Ganesan. 2002. The human homologue of unc-93 maps to chromosome 6q27—characterisation and analysis in sporadic epithelial ovarian cancer. *BMC Genet.* 3:20.

Maehr, R., H.C. Hang, J.D. Mintern, Y.M. Kim, A. Cuvillier, M. Nishimura, K. Yamada, K. Shirahama-Noda, I. Hara-Nishimura, and H.L. Ploegh. 2005. Asparagine endopeptidase is not essential for class II MHC antigen presentation but is required for processing of cathepsin L in mice. *J. Immunol.* 174:7066–7074.

Matsumoto, M., K. Funami, M. Tanabe, H. Oshiumi, M. Shingai, Y. Seto, A. Yamamoto, and T. Seya. 2003. Subcellular localization of Toll-like receptor 3 in human dendritic cells. *J. Immunol.* 171:3154–3162.

Nagai, Y., S. Akashi, M. Nagafuku, M. Ogata, Y. Iwakura, S. Akira, T. Kitamura, A. Kosugi, M. Kimoto, and K. Miyake. 2002. Essential role of MD-2 in LPS responsiveness and TLR4 distribution. *Nat. Immunol.* 3:667–672.

Nishiya, T., and A.L. DeFranco. 2004. Ligand-regulated chimeric receptor approach reveals distinctive subcellular localization and signaling properties of the Toll-like receptors. *J. Biol. Chem.* 279:19008–19017.

Nishiya, T., E. Kajita, S. Miwa, and A.L. Defranco. 2005. TLR3 and TLR7 are targeted to the same intracellular compartments by distinct regulatory elements. *J. Biol. Chem.* 280:37107–37117.

Partridge, A.W., A.G. Therien, and C.M. Deber. 2004. Missense mutations in transmembrane domains of proteins: phenotypic propensity of polar residues for human disease. *Proteins*. 54:648–656.

Poltorak, A., X. He, I. Smirnova, M.Y. Liu, C. Van Huffel, X. Du, D. Birdwell, E. Alejos, M. Silva, C. Galanos, et al. 1998. Defective LPS signaling in C3H/HeJ and C57BL/10ScCr mice: mutations in Tlr4 gene. *Science*. 282:2085–2088.

Randow, F., and B. Seed. 2001. Endoplasmic reticulum chaperone gp96 is required for innate immunity but not cell viability. *Nat. Cell Biol.* 3:891–896.

Shim, J.H., C. Xiao, A.E. Paschal, S.T. Bailey, P. Rao, M.S. Hayden, K.Y. Lee, C. Bussey, M. Steckel, N. Tanaka, et al. 2005. TAK1, but not TAB1 or TAB2, plays an essential role in multiple signaling pathways in vivo. *Genes Dev.* 19:2668–2681.

Shimazu, R., S. Akashi, H. Ogata, Y. Nagai, K. Fukudome, K. Miyake, and M. Kimoto. 1999. MD-2, a molecule that confers lipopolysaccharide responsiveness on Toll-like receptor 4. *J. Exp. Med.* 189:1777–1782.

Spooner, R.A., D.C. Smith, A.J. Easton, L.M. Roberts, and J.M. Lord. 2006. Retrograde transport pathways utilised by viruses and protein toxins. *Virol. J.* 3:26.

Suzuki, N., S. Suzuki, G.S. Duncan, D.G. Millar, T. Wada, C. Mirtsos, H. Takada, A. Wakeham, A. Itie, S. Li, et al. 2002. Severe impairment of interleukin-1 and Toll-like receptor signalling in mice lacking IRAK-4. *Nature*. 416:750–756.

Tabeta, K., P. Georgel, E. Janssen, X. Du, K. Hoebe, K. Crozat, S. Mudd, L. Shamel, S. Sovath, J. Goode, et al. 2004. Toll-like receptors 9 and 3 as essential components of innate immune defense against mouse cytomegalovirus infection. *Proc. Natl. Acad. Sci. USA*. 101:3516–3521.

Tabeta, K., K. Hoebe, E.M. Janssen, X. Du, P. Georgel, K. Crozat, S. Mudd, N. Mann, S. Sovath, J. Goode, et al. 2006. The Unc93b1 mutation 3d disrupts exogenous antigen presentation and signaling via Toll-like receptors 3, 7 and 9. *Nat. Immunol.* 7:156–164.

Takeda, K., T. Kaisho, and S. Akira. 2003. Toll-like receptors. *Annu. Rev. Immunol.* 21:335–376.